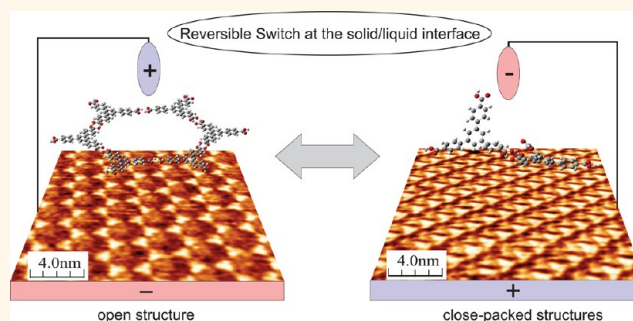


Local Conformational Switching of Supramolecular Networks at the Solid/Liquid Interface

Fernando P. Cometto,^{*,†,‡} Klaus Kern,^{*,§} and Magalí Lingenfelder^{*,†,‡}

[†]Max Planck-EPFL Laboratory for Molecular Nanoscience, and [‡]Institut de Physique de la Matière Condensée, École Polytechnique Fédérale de Lausanne, CH 1015 Lausanne, Switzerland and [§]Max-Planck-Institut für Festkörperforschung, D-70569 Stuttgart, Germany

ABSTRACT We use the electric field in a scanning tunneling microscope to manipulate the transition between open and close packed 2D supramolecular networks of neutral molecules in nonpolar media. We found that while the magnitude of the applied field is not decisive, it is the sign of the polarization that needs to be maintained to select one particular polymorph. Moreover, the switching is independent of the solvent used and fully reversible. We propose that the orientation of the surface dipole determined by the electric field might favor different conformation-dependent charge transfer mechanisms of the adsorbates to the surface, inducing open (closed) structures for negative (positive) potentials. Our results show the use of local fields to select the polymorphic outcome of supramolecular assemblies at the solid/liquid interface. The effect has potential to locally control the capture and release of analytes in host–guest systems and the 2D morphology in multicomponent layers.



KEYWORDS: self-assembly · scanning tunneling microscopy (STM) · phase behavior · molecular switch · surface science

Self-assembled monolayers (SAMs) on surfaces constitute the basis for molecular nanodevices.^{1–4} The tuning of charge transport properties is crucial for molecular electronics and is critically determined by conformation-dependent molecule–surface and molecule–molecule interactions.^{5–19} Ultimately, most applications require the possibility of controlling molecular conformation in a predictable way.^{15,20–29} Thus, different external *stimuli* such as light^{30,31} and temperature^{24,25} have been explored to gain control over the morphology of supramolecular layers.

The local electric field under a scanning tunneling microscope (STM) tip can be used to manipulate the diffusion and arrangement of atoms and molecules at the nanoscale.^{32–41} Because of strong intermolecular interactions that need to be reconfigured to manipulate the intermolecular connectivity landscape, it has been difficult to obtain reversible conformational switching in SAMs by means of electric fields. Accordingly, the systems studied so far included either metal–organic complexes

with high intrinsic dipolar moments that can flip aligning to an external field^{33–35} or ionized species being adsorbed/desorbed or restructured from the solution in response to a charged interface.^{39,40} Specially challenging is the possibility to find robust and reproducible systems that can keep the same response and reversibility after numerous switching cycles.

Herein, we show how the voltage applied *in situ* by a STM can be used to gain full control over the opening and closing of nanoporous structures of a purely organic and neutral molecule: 1,3,5-tris(4-carboxyphenyl) benzene (BTB) on HOPG. The switch is fully reproducible and reverts immediately according to the orientation of the electric field.

RESULTS AND DISCUSSION

In Figure 1 we show STM images of different supramolecular phases of BTB in *n*-nonanoic acid (NA). At very low concentrations (2.5% of a saturated solution = 12.5 μM) we observe an open porous network formed by six BTB molecules

* Address correspondence to fernando.cometto@epfl.ch, magali.lingenfelder@epfl.ch.

Received for review March 17, 2015 and accepted April 8, 2015.

Published online April 10, 2015
10.1021/acsnano.5b01658

© 2015 American Chemical Society

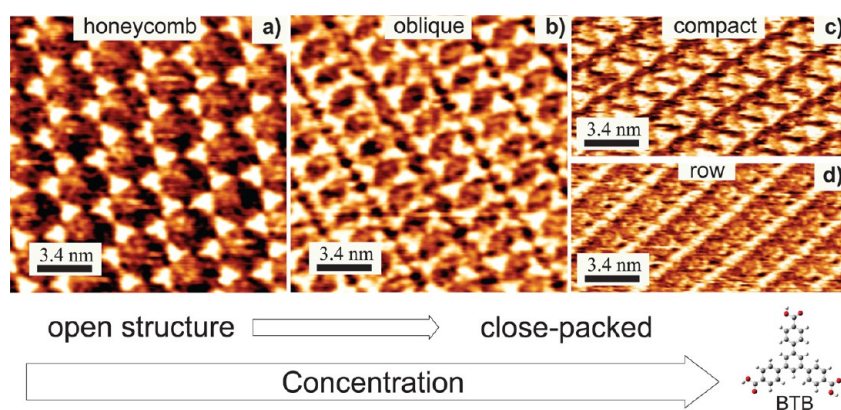


Figure 1. STM images showing the concentration-dependence morphology of BTB monolayers on HOPG at the solid/liquid interface ($V_{\text{bias}} = 850 \text{ mV}$; $I = 150 \text{ pA}$). Typical structure obtained for (a) very diluted solutions ($\leq 12.5 \mu\text{M}$; 2.5% from the saturated solution), (b) diluted solutions ($25 \mu\text{M}$; 5% from the saturated solution) and (c,d) saturated solutions of BTB in NA.

(Figure 1a). In earlier works, this low-density ($0.23 \text{ molecules/nm}^2$) “honeycomb” (also named “chicken-wire”) structure has been the only phase observed in NA at room temperature, for any range of concentrations.^{9,24} Interestingly, in this work we find that also other structures can be produced in NA by careful control of the BTB concentration. By increasing the concentration to 5% ($25 \mu\text{M}$) we obtain the “oblique”¹⁰ structure (Figure 1b). This structure has been previously identified for BTB when using solvents with higher polarity, as in the case of shorter chain length fatty acid solvents.⁹

Gutzler *et al.*²⁴ found a densely packed “row” structure for BTB in NA when heating the substrate to $55 \text{ }^\circ\text{C}$ and also when measuring in *n*-heptanoic acid (HA) at $25\text{--}60 \text{ }^\circ\text{C}$. They modeled the densely packed row structure ($0.87 \text{ molecules/nm}^2$) with the molecules nearly upright, having two carboxylic groups interacting with the surface while the third carboxylic group points off the surface into the solution. In this work we find the row structure at saturated solutions, coexisting with a “compact” phase with lower density ($0.56 \text{ molecules/nm}^2$) (Figure 1c,d and Supporting Information, Figures S1–S2). For concentrations of 10% of dilution ($50 \mu\text{M}$), we observe the expression of all the close-packed phases: oblique, compact, and row (Supporting Information, Figure S2). After some minutes, domain areas become larger by Oswald ripening and after 2h no evidence of other less densely packed structures have been found (Supporting Information, Figure S3).

In literature, there are several works showing the same trend, where less densely packed polymorphs are obtained for diluted solutions.^{13,14,17,24,25} Accordingly, we found a critical concentration (C_0) of $32 \mu\text{M}$ that represents the limit of occurrence of an open (honeycomb) or a densely packed structure at room temperature (Supporting Information, Figure S4) when measuring at positive sample potential.

Other authors have modeled the concentration dependence of bimorphic monolayer self-assembly

in detail and concluded that densely packed polymorphs become thermodynamically preferred at higher solute concentrations.^{14,28} However, we notice that in this system the polymorphic structures show a concentration selection during approximately 1 h, after which they tend to transition toward close packed phases for all ranges of initial concentrations, indicating that open structures are only kinetically favored.²⁶

During all the experiments described above, we always measured at positive sample bias at room temperature. Surprisingly, we found that for freshly deposited solutions we solely observe close-packed structures (for concentrations higher than C_0) when we measure at a positive sample bias. In turn, when we switch the polarity to negative sample bias we detect exclusively the honeycomb structure (Figure 2). Figure 2 panels a–c illustrate the dependence on the sample polarity of a BTB monolayer physisorbed on graphite. Figure 2a shows a typical close-packed structure at a sample bias of $+850 \text{ mV}$; 100 pA (the blue arrow indicates the scanning direction). When a negative sample bias of -850 mV was applied, the more densely packed structure was transformed into the honeycomb structure as indicated in Figure 2b. When the bias potential is maintained at -850 mV the subsequent image (Figure 2c) shows the emergence of a homogeneous honeycomb structure along the scanned area.

This change is induced independently of the BTB concentration (for any concentration higher than C_0). By gradually changing the magnitude of the bias voltage we could establish a window in which the phase change is observed (Figures 2d). The blind region indicates the zone where no measurements are possible due to imaging conditions. It is important to point out that any change in the sign of the sample polarity (from $-1\text{...}-0.35 \text{ V}$ to $+0.4\text{...}+1 \text{ V}$) independently of its magnitude will immediately allow us to observe exclusively one structure. No time

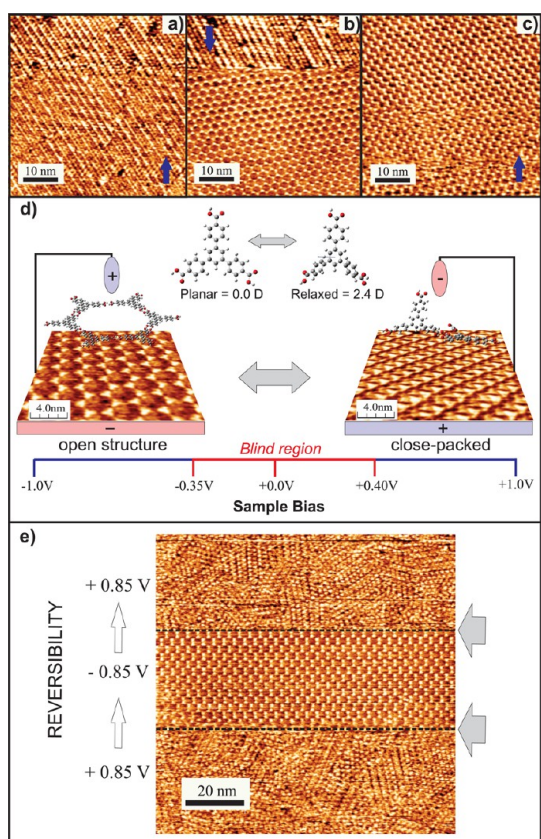


Figure 2. (a–c) Sequential STM images showing the voltage-induced phase transformation. Blue arrows indicate the scan direction (solution = 50 μ M BTB in NA; $I = 100$ pA). (d) Representation of the phase transition with the applied bias-voltage showing the optimized structures of each phase, the calculated intrinsic dipole moment of planar vs relaxed structure in vacuum (top) and the potential region where the phase transition takes place (bottom). (e) STM image showing the reversibility of the phase changes (solution = 5 μ M BTB in NA; $I = 40$ pA).

dependence is evidenced as the transformation always occurs from one scan line to the next one (~ 10 s).

To study the reversibility of this particular process, the bias polarity was changed abruptly from -850 mV \rightarrow $+850$ mV \rightarrow -850 mV in the same scanned area (Figure 2e). The observed transformation of BTB morphology by reverting the electric field direction is highly reproducible, as can be seen in several experiments (see Supporting Information, Figure S5).

Changes in the morphology induced by the STM tip were observed previously in molecular assemblies both at the solid/vacuum³³ and liquid/solid interface.^{34–37,41} Most examples refer to 180° flipping of nonplanar metal naphthalocyanines and noncentrosymmetric triple-decker complexes.^{33–35} In all these cases the molecules had a strong intrinsic molecular dipole that was flipping direction in order to align with the applied electric field. Instead, for BTB one possible scenario involves the molecules in solution being pushed away or aligned with the electric field depending on the polarization at the surface. The fact that the

two polymorphs can coexist on the surface also indicates that their adsorption energies are similar.²⁴ Therefore, the applied electrostatic field might change the delicate balance between molecule–molecule and molecule–surface interactions and favor one conformer over the other. According to our DFT calculations (B3LYP/6311G++), the intrinsic dipole moment P of the optimized structure of BTB is 2.4 D along the central ring (Figure 2d and Supporting Information, Figure S6).

Interestingly, the optimized structure of the honeycomb phase on HOPG is the only structure completely flat on the surface (in order to maximize the H-bonding interactions between neighboring molecules)²⁴ with a resultant dipolar moment of zero (Figure 2d). Thus, molecules adsorbed on the surface in a close-packed less planar structure could allow the molecular dipole to align with the applied electric field. A conformation-dependent charge transfer mechanism is consistent with the presence of two surface active centers, involving both the electrons of the benzene ring (backdonation from the surface to the π -antibonding orbital of the molecule, enhanced in the flat configuration) and the free electron pairs on carboxylic oxygens (donation, enhanced for the upright configuration).⁴² Recent DFT calculations for trimesic acid (TMA) on graphene,⁴³ show that the deformation of COOH groups bending toward the surface affects electron donation and backdonation. The formation of a honeycomb H-bonded network decreases the TMA deformation and the interaction with the surface, while the stability of the adsorbed network is compensated by H bonding.⁴³ This mechanism is also compatible with a partial deprotonation of the BTB molecule being favored under positive surface potential. In contrast to thermal annealing in UHV experiments,²⁹ in solution the presence of a H^+ acceptor is fundamental to allow deprotonation. As autoprotolysis constants of long chain carboxylic acids are very low⁴⁴ and the phase transformation was found to be independent of the polarity of the solvent for *n*-heptanoic acid, *n*-phenyloctane, and *n*-dodecane (Supporting Information, Figure S7), the deprotonation seems unlikely unless a contamination with water traces is present in all the experiments. Moreover, no bias induced transformations were observed for molecules that present only flat conformers on HOPG as melamine and the linear ditopic molecule 4,4''-di(pyridine-4-yl)-1,1':4',1''-terphenyl (BPTB) in NA, indicating that the conformation-dependent dipole of BTB promotes the structural transition.

It is known that the stability of the open structure is related to the coadsorption of solvent molecules in the pores of the network.^{9,24,25} In some images we can even resolve an ordered structure of solvent molecules inside the pores (Supporting Information, Figure S8). Nevertheless, we found that unless a negative surface

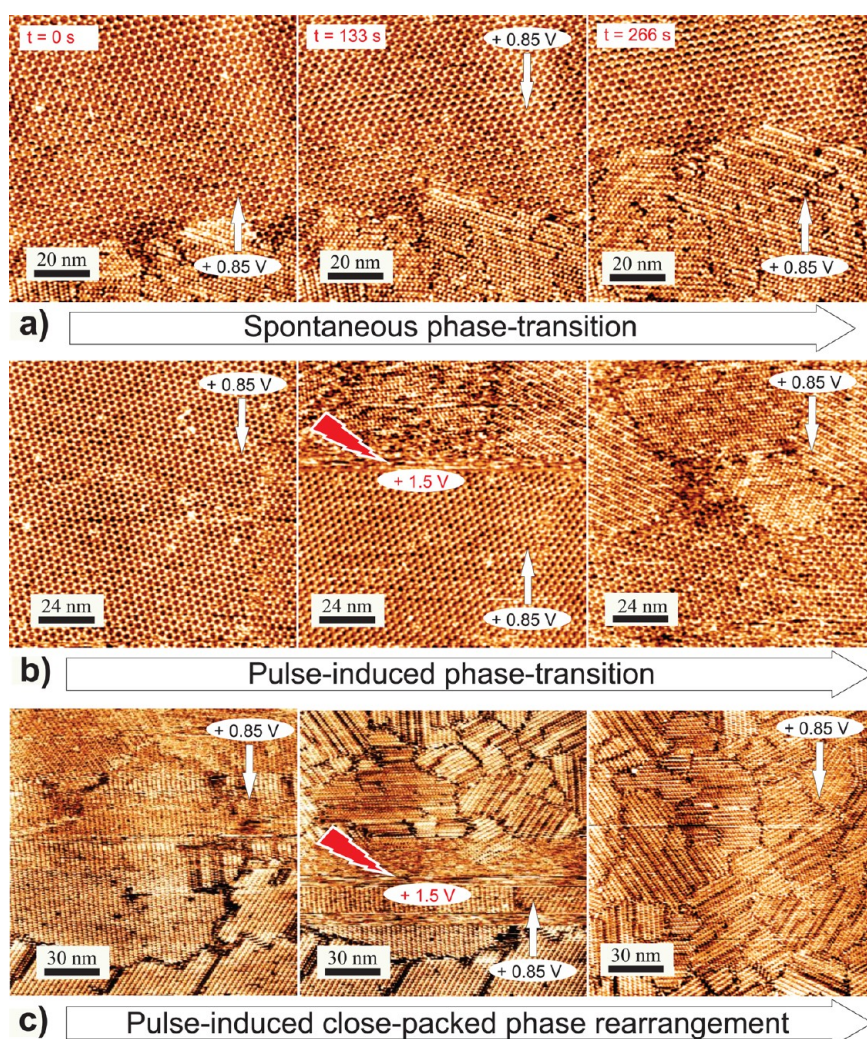


Figure 3. (a) Sequential STM images showing the spontaneous phase transformation (from honeycomb to close-packed structures) of a sample prepared from a very diluted BTB solution ($12.5 \mu\text{M}$). $I = 150 \text{ pA}$. (b) The same phase transformation but induced by a pulse (1.5 V ; 100 ms) of a sample prepared from a very diluted BTB solution ($12.5 \mu\text{M}$). $I = 150 \text{ pA}$. (c) Rearrangement of a close-packed structure induced by a pulse in a saturated BTB solution in NA. $I = 200 \text{ pA}$. White arrows indicate the scan direction.

potential is maintained the honeycomb structure is not stable over long periods of time. In Figure 3a, the spontaneous transformation of a very diluted BTB/NA honeycomb structure into a close-packed structure at room temperature is clearly observed, revealing the instability of this phase. According to our results, the honeycomb phase is kinetically favored in diluted solutions, but it transforms into a denser phase with a small energy barrier. To induce the transformation process, we applied a perturbation (*i.e.*, potential pulses of different magnitude and application time) on the sample. We found that in fresh networks (honeycomb structures obtained immediately after the addition of a very diluted BTB solution on the substrate) a pulse of 1.5 V (100 ms) on the sample is enough to transform a honeycomb into a close-packed structure, Figure 3b). This phase transition induced by a single pulse (without polarity switch) is time dependent upon the initial concentration and it is not directly

reversible; that is, a negative pulse of the same magnitude does not induce the reversal to the original structure. Moreover, the application of a potential pulse (1.5 V ; 100 ms) to the thermodynamically stable structure formed from a saturated BTB solution induced a rearrangement, generating small domain areas of densely packed structures (Figure 3c). This points toward a situation where the pulse provides the energy to desorb the molecules from the surface and at the same time eject molecules toward the surface increasing the local concentration.

In contrast, when we have a close-packed structure prepared from very diluted solutions (1% dilution, $5 \mu\text{M}$) produced after a perturbation or spontaneously formed after 1 h (Figure 4a), the application of a pulse destroys the network and the kinetically favored open structure is immediately formed (Figure 4b,c). Because of the instability of the honeycomb phase under positive sample potential, after some minutes,

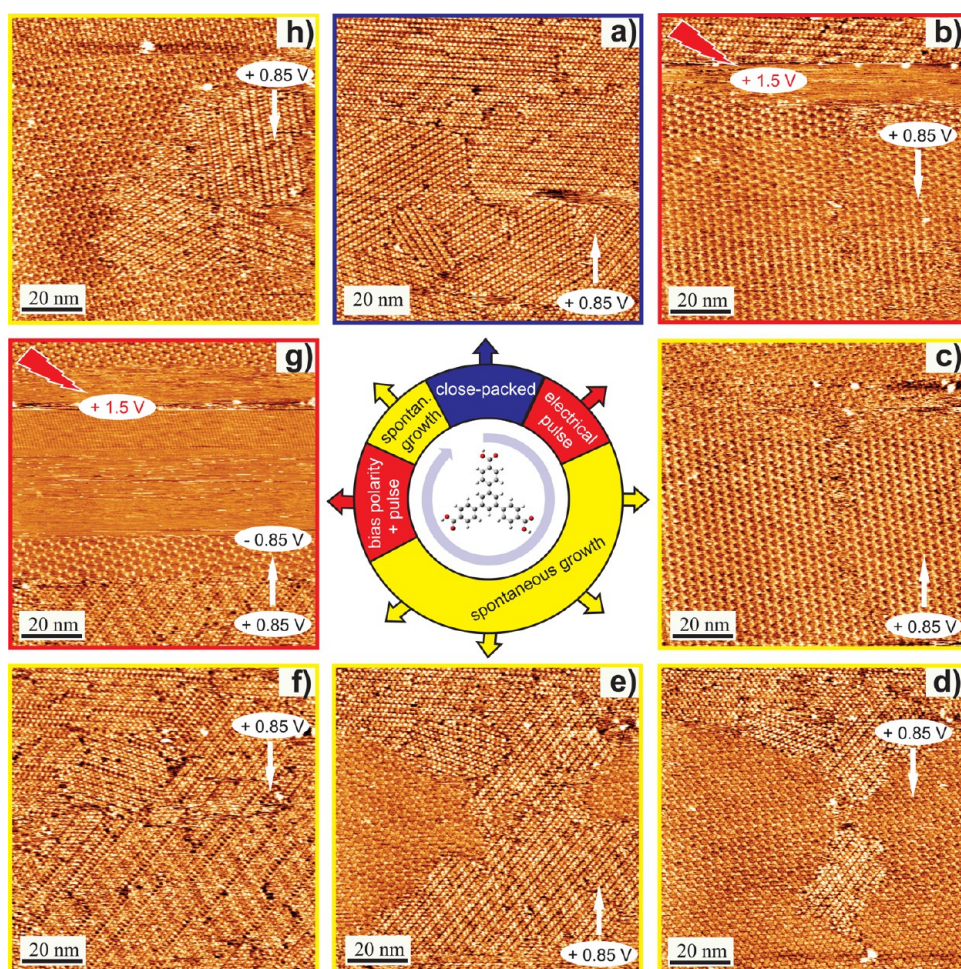


Figure 4. Reversible cycle showed by consecutive STM images on a very diluted BTB solution ($5 \mu\text{M}$) in NA on HOPG: (a) Close-packed structure obtained after 1 h or by a perturbation by an electrical pulse; (b) after the application of an electrical pulse $>1.5 \text{ V}$, the honeycomb structure appears; (c) the honeycomb structure is obtained in the scanned area (kinetically favored structure); (d,e) the close-packed structure grows mostly at defects; (f) the close-packed structure covers the entire scanned surface (thermodynamically favored structure); (g) voltage-induced phase transformation from close-packed to honeycomb structure (bottom) and application of a 1.5 V pulse (top); (h) spontaneous growth of the close-packed structure. $I = 100 \text{ pA}$.

the thermodynamically stable close-packed structure starts to grow preferentially at substrate defects (or domain boundaries) covering the whole surface (Figures 4d–f). As we described above, if we change the sample polarity the open honeycomb structure appears (Figure 4g, bottom). In the case of very diluted solutions, the network is even missed until a new positive pulse is applied (increasing the local concentration) as can be seen in Figure 4g, top. After that the close-packed structure starts to grow again mainly at surface defects and covers the entire scanned surface (Figure 4 h). This particular cycle described in Figure 4 could be repeated several times in the same area.

Another observation that confirms this scenario is that, once a close-packed structure is formed, a decrease in the global BTB concentration in the solution does not revert to the original structure. This effect was proven adding pure solvent during the measurements (not shown).

CONCLUSIONS

The supramolecular assembly of BTB molecules at the liquid/solid interface can be tuned both by the solute concentration (either globally or locally) and by the polarization at the surface–molecule interface. The two tip-induced transformations described here have a different nature. The application of a local pulse causes a gradual rearrangement of molecules toward the thermodynamic polymorphs. The final rearrangement after the pulse depends on the magnitude (extra energy injected in the system) and the initial concentration of the solution. While in the case of a change in the polarization, the magnitude of the change does not play a role, it is the sign of the polarization that needs to be maintained to favor one particular polymorph. This transformation is independent of the solvent and is fully and immediately reverted by changing the sign of the bias voltage. This means that the conformation of the molecules with respect to the surface is directly

determined by the orientation of the surface dipole. In particular, the orientation of the surface dipole under positive voltages might induce COOH groups to bend toward the surface inducing the molecule into a non-planar configuration that allows the molecular dipole to respond to the electric field.

The presented tunable morphology could be used in functional molecular architectures in which nanopores could act as a target site for catalysis, controllable drug release, host–guest chemistry, *etc.* and this capability

could be switched on/off *in situ*. Moreover we are currently using this effect to investigate tunable rearrangements in mixed phases with planar and non-planar adsorbates that respond distinctly to the orientation of the surface dipole, allowing local control of the partial interfacial concentration. In a more general context, we expect this work to draw attention to the “non-innocent” role of the sample polarity in determining the morphological outcome of supramolecular adlayers, even for neutral species in nonpolar media.

EXPERIMENTAL SECTION

Solutions of different concentrations of 1,3,5-tris(4-carboxyphenyl) benzene (BTB) were prepared in *n*-nonanoic acid (synthesis, Merck), *n*-heptanoic acid (98%, Aldrich), *n*-dodecane (synthesis, Merck), and *n*-phenyl octane (98%, Aldrich). Highly ordered pyrolytic graphite (HOPG, Bruker), ZYB grade was used as substrate. The HOPG substrate was cleaved with adhesive tape prior to use. The samples were prepared by depositing 4 μL of BTB solution on the HOPG substrate. STM tips were prepared by mechanical cutting of Pt/Ir wire (90%/10%, diameter 0.25 mm, GoodFellow). All STM measurements were performed using a Bruker system at constant-current mode. After the samples were prepared the tip was immersed in the droplet of solution at the liquid/solid interface. STM images were processed using WSxM 5.0 software.⁴⁵

Conflict of Interest: The authors declare no competing financial interest.

Supporting Information Available: Further STM images showing the reproducibility of the transformation, DFT calculations of the dipolar momentum of different BTB geometries. This material is available free of charge *via* the Internet at <http://pubs.acs.org>.

Acknowledgment. We acknowledge M. Lackinger for experimental advice during the first phase of our work, R. Gutzler for providing the original MD file of the row structure (for comparison), G. Ruano for participating in several discussions, and S. De Feyter for his interest in our project and for many useful discussions. F.P.C. thanks CONICET-Argentina for the “young researchers” scholarship.

REFERENCES AND NOTES

- Barth, J. V.; Costantini, G.; Kern, K. Engineering Atomic and Molecular Nanostructures at Surfaces. *Nature* **2005**, *437*, 671–679.
- Kühnle, A. Self-Assembly of Organic Molecules at Metal Surfaces. *Curr. Opin. Colloid Interface Sci.* **2009**, *14*, 157–168.
- Yang, Y. L.; Wang, C. Solvent Effects on Two-Dimensional Molecular Self-Assemblies Investigated by Using Scanning Tunneling Microscopy. *Curr. Opin. Colloid Interface Sci.* **2009**, *14*, 135–147.
- Kudernac, T.; Lei, S. B.; Elemans, J. A. A. W.; De Feyter, S. Two-Dimensional Supramolecular Self-Assembly: Nanoporous Networks on Surfaces. *Chem. Soc. Rev.* **2009**, *38*, 402–421.
- Tseng, T.-C.; Urban, C.; Wang, Y.; Otero, R.; Tait, S. L.; Alcamí, M.; Écija, D.; Trelka, M.; Gallego, J. M.; Lin, N.; *et al.* Charge-Transfer-Induced Structural Rearrangements at Both Sides of Organic/Metal Interfaces. *Nat. Chem.* **2010**, *2*, 374–379.
- Klappenberger, F.; Cañas-Ventura, M. E.; Clair, S.; Pons, S.; Schlickum, U.; Qu, Z. R.; Strunskus, T.; Comisso, A.; Wöll, C.; Brune, H.; *et al.* Does the Surface Matter? Hydrogen-Bonded Chain Formation of an Oxalic Amide Derivative in a Two- and Three-Dimensional Environment. *ChemPhysChem* **2008**, *9*, 2522–2530.
- Kampschulte, L.; Werblowsky, T. L.; Kishore, R. S. K.; Schmittl, M.; Heckl, W. M.; Lackinger, M. Thermodynamical Equilibrium of Binary Supramolecular Networks at the Liquid–Solid Interface. *J. Am. Chem. Soc.* **2008**, *130*, 8502–8507.
- Gutzler, R.; Lappe, S.; Mahata, K.; Schmittl, M.; Heckl, W. M.; Lackinger, M. Aromatic Interaction vs Hydrogen Bonding in Self-Assembly at the Liquid–Solid Interface. *Chem. Commun.* **2009**, *6*, 680–682.
- Kampschulte, L.; Lackinger, M.; Maier, A. K.; Kishore, R. S. K.; Griessl, S.; Schmittl, M.; Heckl, W. M. J. Solvent Induced Polymorphism in Supramolecular 1,3,5-Benzenetribenzoic Acid Monolayers. *Phys. Chem. B* **2006**, *110*, 10829–10836.
- Silly, F. Two-Dimensional 1,3,5-Tris(4-carboxyphenyl) benzene Self-Assembly at the 1-Phenyl octane/Graphite Interface Revisited. *Phys. Chem. C* **2012**, *116*, 10029–10032.
- Mamdouh, W.; Uji-i, H.; Ladislav, J. S.; Dulcey, A. E.; Percec, V.; De Schryver, F. C.; De Feyter, S. Solvent Controlled Self-Assembly at the Liquid–Solid Interface Revealed by STM. *J. Am. Chem. Soc.* **2006**, *128*, 317–325.
- Li, Y. B.; Ma, Z.; Qi, G. C.; Yang, Y. L.; Zeng, Q. D.; Fan, X. L.; Wang, C.; Huang, W. J. Toward the Rational Design of Supramolecular Coordination Polymers. The Effect of Solvent and Substituent Changes on the Structure of Self-Assembled Metal–Organometallic Networks. *Phys. Chem. C* **2008**, *112*, 8649–8653.
- Zhang, X.; Chen, Q.; Deng, G. J.; Fan, Q. H.; Wan, L. J. J. Structural Diversity of a Monodendron Molecule Self-Assembly in Different Solvents Investigated by Scanning Tunneling Microscopy: From Dispersant to Counterpart. *Phys. Chem. C* **2009**, *113*, 16193–16198.
- Lei, S. B.; Tahara, K.; De Schryver, F. C.; Van der Auweraer, M.; Tobe, Y.; De Feyter, S. One Building Block, Two Different Supramolecular Surface-Confined Patterns: Concentration in Control at the Solid–Liquid Interface. *Angew. Chem., Int. Ed.* **2008**, *47*, 2964–2968.
- Palma, C. A.; Bjork, J.; Bonini, M.; Dyer, M. S.; Llanes-Pallas, A.; Bonifazi, D.; Persson, M.; Samorí, P. Tailoring Bicomponent Supramolecular Nanoporous Networks: Phase Segregation, Polymorphism, and Glasses at the Solid–Liquid Interface. *J. Am. Chem. Soc.* **2009**, *131*, 13062–13071.
- Lackinger, M.; Heckl, W. M. Carboxylic Acids: Versatile Building Blocks and Mediators for Two-Dimensional Supramolecular Self-Assembly. *Langmuir* **2009**, *25*, 11307–11321.
- Ha, N. T. N.; Gopakumar, T. G.; Hietschold, M. Polymorphism Driven by Concentration at the Solid–Liquid Interface. *J. Phys. Chem. C* **2011**, *115*, 21743–21749.
- Ha, N. T. N.; Gopakumar, T. G.; Gutzler, R.; Lackinger, M.; Tang, H.; Hietschold, M. J. Influence of Solvophobic Effects on Self-Assembly of Trimesic Acid at the Liquid–Solid Interface. *Phys. Chem. C* **2010**, *114*, 3531–3536.
- Ha, N. T. N.; Gopakumar, T. G.; Hietschold, M. Polymorphs of Trimesic Acid Controlled by Solvent Polarity and Concentration of Solute at Solid–Liquid Interface. *Surf. Sci.* **2013**, *607*, 68–73.
- Bleger, D.; Kreher, D.; Mathevet, F.; Attias, A. J.; Schull, G.; Huard, A.; Douillard, L.; Fiorini-Debuschert, C.; Charra, F. Surface Noncovalent Bonding for Rational Design of

- Hierarchical Molecular Self-Assemblies. *Angew. Chem., Int. Ed.* **2007**, *46*, 7404–7407.
21. English, W. A.; Hippos, K. W. Stability of a Surface Adlayer at Elevated Temperature: Coronene and Heptanoic Acid on Au(111). *J. Phys. Chem. C* **2008**, *112*, 2026–2031.
 22. Kong, X. H.; Deng, K.; Yang, Y. L.; Zeng, Q. D.; Wang, C. Effect of Thermal Annealing on Hydrogen Bond Configurations of Host Lattice Revealed in VOPc/TCDB Host–Guest Architectures. *J. Phys. Chem. C* **2007**, *111*, 9235–9239.
 23. Li, C. J.; Zeng, Q. D.; Liu, Y. H.; Wan, L. J.; Wang, C.; Wang, C. R.; Bai, C. L. Evidence of a Thermal Annealing Effect on Organic Molecular Assembly. *ChemPhysChem* **2003**, *4*, 857–859.
 24. Gutzler, R.; Sirtl, T.; Dienstmaier, J. F.; Mahata, K.; Heckl, W. M.; Schmittel, M.; Lackinger, M. Reversible Phase Transitions in Self-Assembled Monolayers at the Liquid–Solid Interface: Temperature-Controlled Opening and Closing of Nanopores. *J. Am. Chem. Soc.* **2010**, *132*, 5084–5090.
 25. Blunt, M. O.; Adisojoso, J.; Tahara, K.; Katayama, K.; Van der Auweraer, M.; Tobe, Y.; De Feyter, S. Temperature-Induced Structural Phase Transitions in a Two-Dimensional Self-Assembled Network. *J. Am. Chem. Soc.* **2013**, *135*, 12068–12075.
 26. Bellec, A.; Arrigoni, C.; Schull, G.; Douillard, L.; Fiorini-Debuisschert, C.; Mathevet, F.; Kreher, D.; Attias, A. J.; Charra, F. Solution-Growth Kinetics and Thermodynamics of Nanoporous Self-Assembled Molecular Monolayers. *J. Chem. Phys.* **2011**, *134*, 124702–124708.
 27. Hirsch, B. E.; McDonald, K. P.; Qiao, B.; Flood, A. H.; Tait, S. L. Selective Anion-Induced Crystal Switching and Binding in Surface Monolayers Modulated by Electric Fields from Scanning Probes. *ACS Nano* **2014**, *8*, 10858–10869.
 28. Meier, C.; Roos, M.; Künzel, D.; Breitruck, A.; Hoster, H. E.; Landfester, K.; Gross, A.; Behm, R. J.; Ziener, U. Concentration and Coverage Dependent Adlayer Structures: From Two-Dimensional Networks to Rotation in a Bearing. *J. Phys. Chem. C* **2010**, *114*, 1268–1277.
 29. Ruben, M.; Payer, D.; Landa, A.; Comisso, A.; Gattinoni, C.; Lin, N.; Collin, J.-P.; Sauvage, J.-P.; De Vita, A.; Kern, K. 2D Supramolecular Assemblies of Benzene-1,3,5-triyl-tribenzoic Acid: Temperature-Induced Phase Transformations and Hierarchical Organization with Macrocyclic Molecules. *J. Am. Chem. Soc.* **2006**, *128*, 15644–15651.
 30. Shen, Y. T.; Guan, L.; Zhu, X. Y.; Zeng, Q. D.; Wang, C. Submolecular Observation of Photosensitive Macrocycles and Their Isomerization Effects on Host–Guest Network. *J. Am. Chem. Soc.* **2009**, *131*, 6174–6180.
 31. Shen, Y. T.; Deng, K.; Zhang, X. M.; Feng, W.; Zeng, Q. D.; Wang, C.; Gong, J. R. Switchable Ternary Nanoporous Supramolecular Network on Photo-regulation. *Nano Lett.* **2011**, *11*, 3245–3250.
 32. Carpinelli, J. M.; Swartzentruber, B. S. Direct measurement of field effects on surface diffusion. *Phys. Rev. B* **1998**, *58*, R13423–R13425.
 33. Gopakumar, T. G.; Müller, F.; Hietschold, M. Scanning Tunneling Microscopy and Scanning Tunneling Spectroscopy Studies of Planar and Nonplanar Naphthalocyanines on Graphite (0001). Part 1: Effect of Nonplanarity on the Adlayer Structure and Voltage-Induced Flipping of Nonplanar Tin–Naphthalocyanine. *J. Phys. Chem. B* **2006**, *110*, 6051–6059.
 34. Lei, S.-B.; Deng, K.; Yang, Y.-L.; Zeng, Q.-D.; Wang, C.; Jiang, J.-Z. Electric Driven Molecular Switching of Asymmetric Tris(phthalocyaninato) Lutetium Triple-Decker Complex at the Liquid/Solid Interface. *Nano Lett.* **2008**, *8*, 1836–1843.
 35. Kong, X.; Lei, S.; Yang, Y.; Deng, K.; Qi, G.; Wang, C. Identification of Molecular Flipping of an Asymmetric Tris(phthalocyaninato) Lutetium Triple-Decker Complex by Scanning Tunneling Microscopy/Spectroscopy. *Nano Res.* **2009**, *2*, 235–241.
 36. Lee, S.-L.; Hsu, Y.-J.; Wu, H.-J.; Lin, H.-A.; Hsu, H.-F.; Chen, C.-h. Electrical Pulse Triggered Reversible Assembly of Molecular Adlayers. *Chem. Commun.* **2012**, *48*, 11748–11750.
 37. Yang, Y.-L.; Chan, Q.-L.; Ma, X.-J.; Deng, K.; Shen, Y.-T.; Feng, X.-Z.; Wang, C. Electrical Conformational Bistability of Dimesogen Molecules with a Molecular Chord Structure. *Angew. Chem., Int. Ed.* **2006**, *45*, 6889–6893.
 38. Qiu, X. H.; Nazin, G. V.; Ho, W. Mechanisms of Reversible Conformational Transitions in a Single Molecule. *Phys. Rev. Lett.* **2004**, *93*, 196806.
 39. Yoshimoto, S.; Sawaguchi, T.; Su, W.; Jiang, J.; Kobayashi, N. Superstructure Formation and Rearrangement in the Adlayer of a Rare-Earth-Metal Triple-Decker Sandwich Complex at the Electrochemical Interface. *Angew. Chem., Int. Ed.* **2007**, *46*, 1071–1074.
 40. Cui, K.; Mali, K. S.; Ivasenko, O.; Wu, D.; Feng, X.; Walter, M.; Mullen, K.; De Feyter, S.; Mertens, S. F. Squeezing, Then Stacking: From Breathing Pores to Three-Dimensional Ionic Self-Assembly under Electrochemical Control. *Angew. Chem., Int. Ed.* **2014**, *53*, 12951–12954.
 41. Mali, K. S.; Wu, D.; Feng, X.; Müllen, K.; Van der Auweraer, M.; De Feyter, S. Scanning Tunneling Microscopy-Induced Reversible Phase Transformation in the Two-Dimensional Crystal of a Positively Charged Discotic Polycyclic Aromatic Hydrocarbon. *J. Am. Chem. Soc.* **2011**, *133*, 5686–5688.
 42. Zelenay, P.; Waszczuk, P.; Dobrowolska, K.; Sobkowski, J. Adsorption of Benzoic Acid on a Polycrystalline Gold Electrode. *Electrochim. Acta* **1994**, *39*, 655–660.
 43. Shayeganfar, F.; Rochefort, A. Electronic Properties of Self-Assembled Trimesic Acid Monolayer on Graphene. *Langmuir* **2014**, *30*, 9707–9716.
 44. Rondinini, S.; Longhi, P.; Mussini, P. R.; Mussini, T. Autoprotolysis Constants in Nonaqueous Solvents and Aqueous Organic Solvent Mixtures. *Pure Appl. Chem.* **1987**, *59*, 1693–1702.
 45. Horcas, I.; Fernández, R.; Gómez-Rodríguez, J. M.; Colchero, J.; Gómez-Herrero, J.; Baro, A. M. WSXM: A Software for Scanning Probe Microscopy and a Tool for Nanotechnology. *Rev. Sci. Instrum.* **2007**, *78*, 013705.